



encit 2020



18<sup>th</sup> Brazilian Congress of Thermal Sciences and Engineering  
November 16-20, 2020 (Online)

ENC-2020-0276

## COMPUTATIONAL ANALYSIS OF SLURRY DRYING THROUGH FILTRATION USING CFD-DEM COUPLED METHODS

**Matheus Dutra Baptista Oliveira**  
**Matheus Felipe Rodrigues Moreira**  
**Cristiana Brasil Maia**

Mechanical engineering department – Pontifícia Universidade Católica de Minas Gerais - Belo Horizonte, Minas Gerais, Brazil.  
matheus.mdbo@gmail.com  
mfelipe17@gmail.com  
cristiana@pucminas.br

**Abstract.** *Computational analysis is performed with the objective to virtually represent objects and equipment's real physical behavior. With simulation is possible to make geometrical and numerical modifications reaching the most efficient operational parameters of the equipment before its fabrication. A CFD-DEM coupled in one-way analysis join two distinct methods of calculation in a single solver, evaluating the iterations between fluid and particles. This article uses the CFD-DEM coupled analysis studying a filtration equipment that transport slurry (fluid + particles) to different exits. A rotational valve restraining the main exit, creates a raising pressure location forcing the slurry to go through a porosity region, with the objective to reduce the number of particles in the exiting water. It was possible to notice the behavior expected, as the influence of fluid in particles motion and the possibility to visualize the slurry flow to the exits, showing the regions where the slurry flow has preference to go through. Good visual results are demonstrated, indicating where the porosity media needs to be cleaned with more frequency avoiding clog.*

**Keywords:** CFD, DEM, DPM, One-way coupling, Porosity

### 1. INTRODUCTION

Even being a pre-historic process, drying still going through constant innovation and researches, principally because of its enormous area of application. According to (MUJUMDAR, 2004), only in the 90's decade in the USA, almost 240 patents were issued per year containing drying processes or drying equipment. The European Office issues 80 patents a year related to the same subject. A lot of energy is consumed by drying processes, what justify the constant research for improvements, especially when dealing with its application in large industrial companies. (HALL, 1988) explains in his text that the efficiency of drying should be measured to satisfy the product application. In some cases, the excessive drying is prejudicial for transportation and storage.

Recent studies apply phase separation processes, not only for drying, looking for different objectives. (LIN; TAI, 2010) uses the separation process to recover silicon powder from the slurry produced when cutting silicon ingots. This process avoids the waste of material and environment contamination. It uses two types of separation, with acid washing and with oil injection, reaching 71,1% of silicone recovery. (JORGENSEN et al., 2010) apply different types of phase separation methodologies in its study, as a purely mechanical separation, separation with utilization of flocculants, anaerobic separation, and centrifugal separation. The results indicate the percentage of solid phosphor in the filtrated slurry. (HAMELIN et al., 2011) uses the phase separation methodology to evaluate the production of biogas. Two types of separation are considered, separation through centrifugal force and screw press separation. Results show that the centrifugal separation is more efficient in biogas production, with 87% of efficiency.

Computational analysis was developed aiming the extraction of physical results through advanced calculation methods, where project modifications could be executed in CAD geometries, what if executed in physical equipment would generate costs. In the past years the power of computational processing got improved, allowing the implementation of a greater number of equations to be solved in a shorter space of time. Analysis through Computational fluid dynamics (CFD) and Discrete element (DEM) methods, has a considerable number of equations to be solved. When the two methods are coupled, the interaction between the results is desirable, increasing considerable the number of equations and resulting in adding processing consumption. Recent papers adopt these methods coupling as (MA et al., 2015) that used CFD and DEM through DPM (Discrete phase model) to visualize the particles motion in accordance with the fluid flow. The DPM

method do not consider the particle-particle neither particle-wall iteration. In other side, (FATAHI; FARZANEGAN, 2018) uses the CFD and DEM through DDPM (Dense discrete phase model) coupling in a four-way analysis that consider the iteration of particle-particle, fluid-particle and particle-fluid, providing more accurate results, because the particles motion also interfere in fluid motion. The analysis was performed for a Knelson separator, and the results were validated with experimental data.

Some authors apply the CFD-DEM coupling to evaluate multiphase fluids flow through fibrous media, with the objective to comprehend the effect of particles deposition in the loss of pressure, and other parameters as well. For exemplification (YUE; ZHANG; ZHAI, 2016) elaborated a 3D model based in a structure of glass fiber to simulate gas and particles flow through it. The CFD-DEM coupled methods were adopted for this simulation, with the objective of evaluate the filter efficiency when parameters as flow velocity, particles diameter and fibers thickness suffer variations. (NGUYEN; INDRARATNA, 2016) couple CFD-DEM methods evaluating the hydraulic flow through natural fibers, for being a natural source, biodegradable and hydraulic conductor. DEM method was adopted to create the connected fibers in linear and spiral arrangement, while CFD method described the fluid flow passing through fibers.

The present article considers a simulation of a drying through filtering equipment witch, by the pressure of slurry column pulls the material against a porosity layer, responsible for retaining a percentage of particles, resulting in separating the solid from liquid phase. The simulation was performed with CFD-DPM one-way analysis and aim in visualize the fluid and particles flow through the internal region of the equipment. CFD-DEM coupling (FERNANDES et al, 2018) considers the equations of Navier-Stokes for fluid phase and Newton's second law of motion for the particles. The equations will be better described in the methodology topic of this paper.

## 2. METHODOLOGY

### 2.1 Computational fluid dynamics (CFD)

Considering a slurry flow, according to (MANNHEIMER, 1991), Reynolds number should be less than 4600 for laminar and above 5000 for turbulent behavior, where it could be calculated through equation (1).

$$Re = \frac{\rho v D}{\mu} \quad (1)$$

Where,

$\rho$ = Fluid specific mass;

$v$ =Fluid velocity;

$D$ =Pipe diameter;

$\mu$ =Fluid viscosity

According to (VERSTEEG; MALALASEKERA, 2007) the laws of mass and momentum conservation are described by equations (2) and (3).

$$\frac{\partial \rho}{\partial t} + \rho \cdot \nabla u = 0 \quad (2)$$

$$\rho \left( \frac{\partial u}{\partial t} + \rho \cdot \nabla u \right) = -\nabla P + \mu_{eq} \nabla^2 u + S \quad (3)$$

Where,

$t$ = Time;

$u$ =Flow velocity;

$p$ =Pressure;

$\mu_{eq}$ = Dynamic equivalent viscosity;

$S$ =Source term.

As (JANUÁRIO; MAIA, 2019) describes, to represent the turbulence behavior, many models could be used, but for this work was selected the k- $\epsilon$ , represented by the equations (4), (5) and (6).

$$\mu_t = \rho C_\mu \frac{k^2}{\epsilon} \quad (4)$$

$$\frac{\partial \rho k}{\partial t} + \frac{\partial \rho k u_i}{\partial x_i} = \frac{\partial}{\partial x_i} \left( \frac{\mu_t}{\sigma_k} \frac{\partial k}{\partial x_i} \right) + 2\mu_t E_{ij} E_{ij} - \rho \epsilon \quad (5)$$

$$\frac{\partial \rho \epsilon}{\partial t} + \frac{\partial \rho \epsilon u_i}{\partial x_j} = \frac{\partial}{\partial x_j} \left( \frac{\mu_t}{\sigma_\epsilon} \frac{\partial \epsilon}{\partial x_j} \right) + C_{1\epsilon} \frac{\epsilon}{k} 2\mu_t E_{ij} E_{ij} - C_{2\epsilon} \rho \frac{\epsilon^2}{k} \quad (6)$$

Where,

$\mu_t$  = Turbulent viscosity;

$C_{\mu}$ ,  $C_{1\epsilon}$ ,  $C_{2\epsilon}$ ,  $\sigma_k$  and  $\sigma_\epsilon$  = Model constants.

$E_{ij}$  = Rate of deformation components

## 2.2 Coupling CFD-DEM

The union of two analysis methods, when applied in a transient simulation, could be made using the information of one of the methods solution (MOHAMMAD et al, 2014) and passing the results to the other, while the second method do not send information to the first one, process called one-way coupling. The one-way coupling process (MOHAMMAD et al, 2014) has a good application when the second method has a relatively small influence in the first one. When the influence between the two methods must be considered, a two-way coupling must be considered. In this kind of coupling, the results of the second method are also used to the first, creating more accuracy to the results.

The discrete phase is governed by Newton's law equations (QIAN et al, 2014) of motion, and could be calculated by:

$$m_p \frac{du_{p,i}}{dt} = F_{g,i} + F'_{fp,i} + F_{nc,i} + f_{n,i} + f_{t,i} \quad (7)$$

$$I_p \frac{d\omega_i}{dt} = T_i \quad (8)$$

Where:

$m_p$  = particle mass

$u_{p,i}$  = speed

$\omega_i$  = angular speed

$f_{n,i}$  = normal collision force

$f_{t,i}$  = tangential collision force

$T_i$  = collision torque

$I_p$  = moment of inertia of particle

$F_{g,i}$  = gravity force

$F'_{fp,i}$  = fluid force

$F_{nc,i}$  = non-contact force

The equation (FERNANDES et al, 2018) that govern the particle-fluid interaction is:

$$F_i^f = F_d + F_{\nabla p} + F_{\nabla \cdot \tau} + F_{vm} + F_B + F_{Saff} + F_{Mag} \quad (9)$$

Where:

$F_i^f$  = particle-fluid interaction term

$F_d$  = drag force

$F_{\nabla p}$  = pressure gradient force

$F_{\nabla \cdot \tau}$  = viscous force

$F_{vm}$  = virtual mass force

$F_B$  = Basset force

$F_{Saff}$  = Saffman force

$F_{Mag}$  = Magnus force

In this paper are considered only the drag force, pressure gradient force and virtual mass force. As in this work the particles and fluid flow is applied in a region of porosity, the equations of a laminar flow with porous media, and no heat exchange, are basically (QIAN et al, 2014) the continuity and momentum ones, expressed as:

$$\frac{\partial \epsilon}{\partial t} + \nabla \cdot (\epsilon u) = 0 \quad (10)$$

$$\frac{\partial}{\partial t}(\rho_f \epsilon u) + \nabla \cdot (\rho_f \epsilon u u) = -\epsilon \nabla P - F_{fp} + \nabla \cdot (\epsilon \tau) + \rho_f \epsilon g \quad (11)$$

Where:

$\epsilon$  = porosity of fibrous media

$u$  = average fluid velocity

$\rho$  = fluid density

$P$  = pressure

$\tau$  = fluid viscosity stress tensor

$F_{fp}$  = interaction forces between the particles

### 3. MATERIALS AND METHOD

This simulation was created with the objective of predict the particles behavior inside a fluid while going through equipment composed by a porous media region. In the physical model (Figure 1), the porous media is responsible to retain a percentage of particles, while the other percentage goes through it. With the complexity of create a geometry of porous media, because of the porous scale relative to the equipment, a pressure loss is considered in porous media region, representing the physical behavior of fluid.



Figure 1. Physical model

The mesh (Figure 2) was created in a surface with only 2D elements. The total number of elements was 91993 while 98,5% were quadratic and the others triangular. Mesh was divided in 4 different zones, slurry zone, purified water zone and porosity zone, according to figure 3. All the mentioned zones were water domain, while the porosity is a water domain with a specified porosity value, aiming to retain or deviate particles. The boundary conditions described in Figure 3 were associated with the related elements in mesh and the numerical parameters were considered according to Table 1.

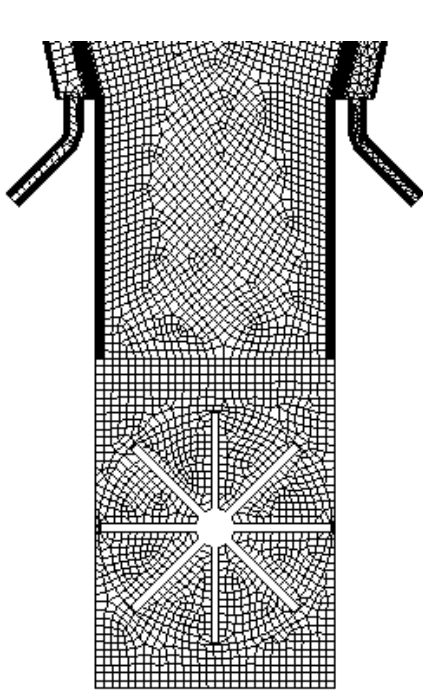


Figure 2. Mesh elements

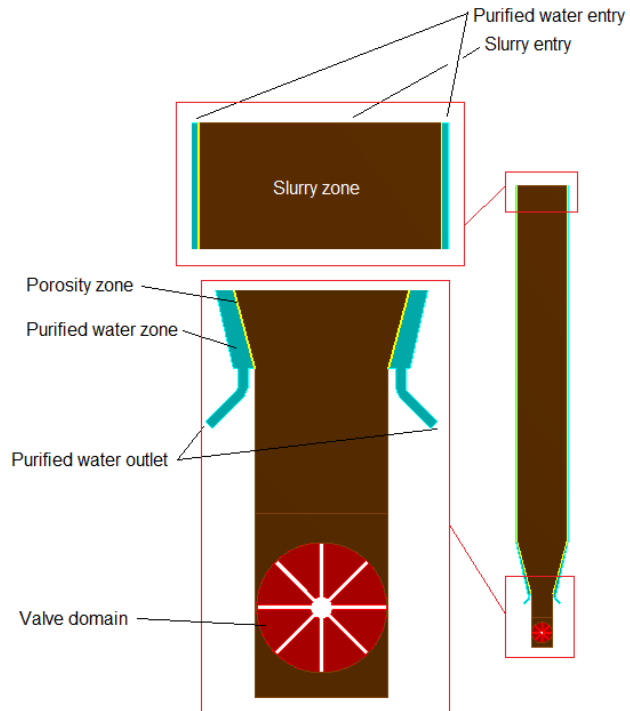


Figure 3. Domain zones

Table 1. Boundary conditions

Parameter	Region	Value
Velocity inlet	Slurry entry	0.1 m/s
Pressure inlet	Purified water entry	1 atm
Pressure outlet	Purified water outlet	1 atm
Pressure outlet	Slurry outlet	1 atm
Rotational velocity	Valve domain	1 rad/s
Wall rough	External wall	0.5
Fluid porosity	Porous region	1
Porosity – Viscous resistance	Porous region	21111000

Reynolds number was calculated (1) and its resultant value of 139.330 exceeds the laminar range, so the k- $\epsilon$  turbulence method was used in the analysis.

The CFD-DEM coupling was performed using the standard formulation of the Lagrangian multiphase discrete phase mode (DPM), that according to (FATAHI; FARZANEGAN, 2018) do not calculate the particle-particle interaction as for example particle's collision. This formulation is most used for a low fraction of particles, what in consequence consumes a lower processing time. Particles were considered massless with a virtual mass physical model, what also do not consider them diameter. A one-way coupling was performed, because as (STONE et al, 2019) describes, a two-way coupling do not affect the deposition of the particles, so it has no effect in an analysis of a one direction flow, as performed in this article.

The simulation was performed in a transient regime with total time of 20 seconds, defined in function of the 200 time steps with a 0,01 time step. As considered in (FATAHI; FARZANEGAN, 2018), a first-order upwind scheme was performed in the volume finite method (VFM), which considers (ANSYS, no date) the cells center values for element's faces. A SIMPLE algorithm was set to this simulation to, according to (ANSYS, no date) maintain a more conservative under-relaxation value, while a turbulence model is being performed.

#### 4. RESULTS

Results were obtained separately for the fluid flow and particles motion. First the fluid flow will be discussed, and after the particles. In Figure 4 is possible to analyze the fluid motion trough the domain in 5 different stages, 2, 8, 12, 17 and 20 seconds. The color scale represents the fluid velocity. Equations (4), (5) and (6) were adopted to calculate the fluid turbulence while Eq. (2) and (3) describes the fluid momentum and mass conservation. It is possible to notice the raise of

central velocity in comparison with wall velocity. This difference is obtained in consequence of the rough promoted by porosity region, creating a boundary layer.

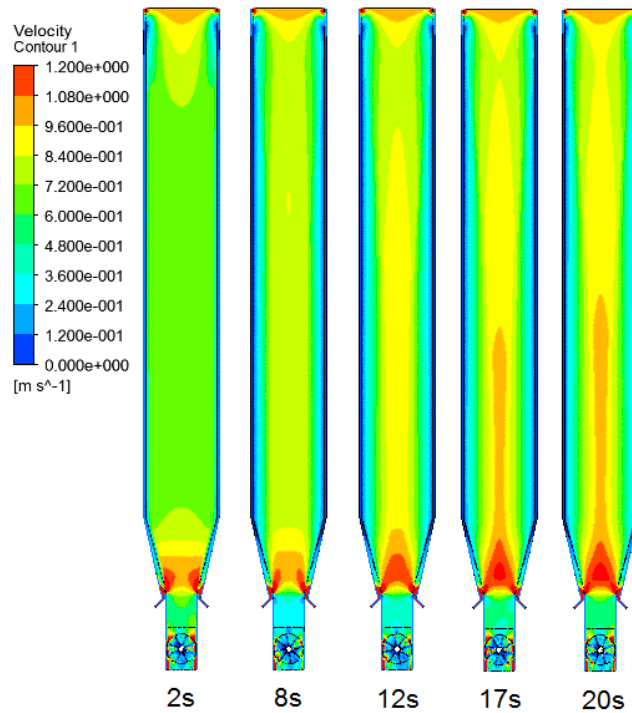


Figure 4. Fluid velocity

In Figure 5 is possible to see the fluid streamlines close to the fluid exits. The streamlines represent the fluid trajectory and its punctual velocity on its way. The restriction promoted by the valve in the main exit, forces the fluid to flow to the purified water exits, passing through the porosity region. This behavior is expected, reaching the objective of redirect the fluid and retain particles in porous area.

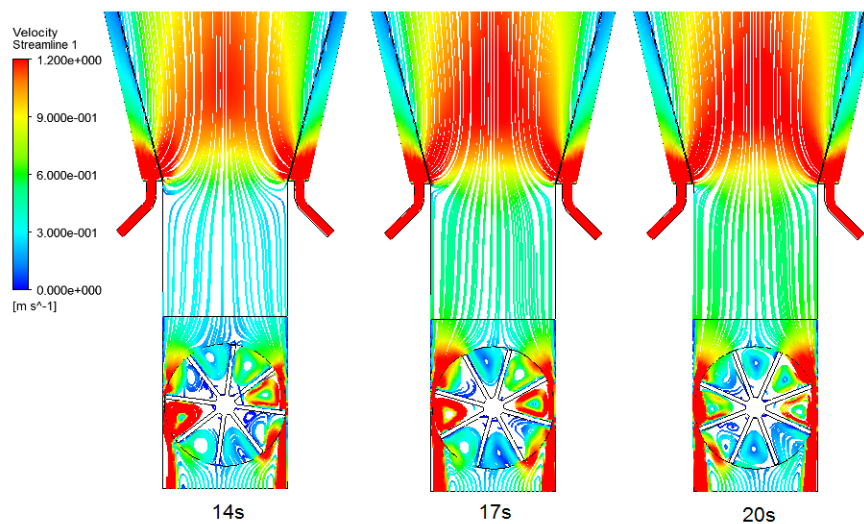


Figure 5. Fluid velocity near to the exit

In sequence the particles results were obtained. In Figure 6 the particles track line was represented with a color scale relative to its velocities. Just like the fluid phase, 5 stages were represented, 2, 8, 12, 17 and 20 seconds. As particles are in a flow determined from fluid's motion with a porosity regions, two groups of equations were adopted, where Eq. (7) and (8) describes the particles motion while Eq. (10) and (11) represent the interference of porosity in fluid and particles'

motion. It's possible to note that the 20s of simulation wasn't enough for that the particles could fill the whole region, although it's evident that the particles flow exactly as the fluid, what is expected in a one way analysis.

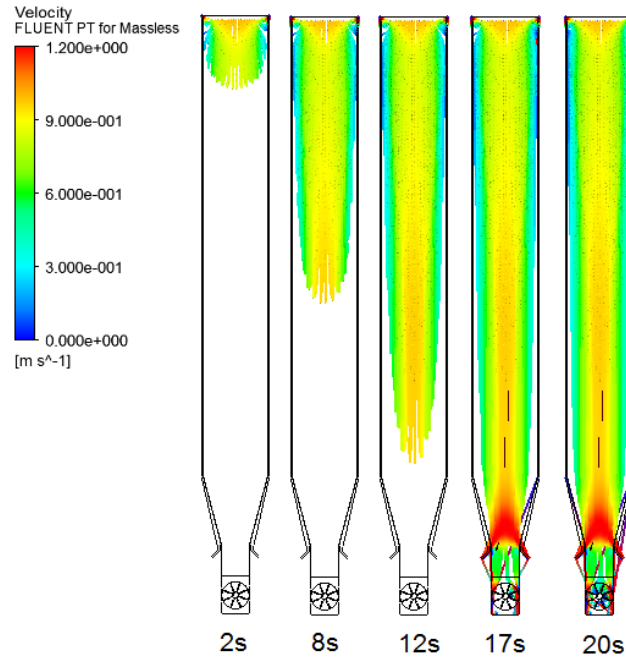


Figure 6. Particles velocity

Aiming a good particle track visualization in the most complex region of the equipment, Figure 7 were inserted to show with more precision the region of particles exit from the system. Through the images, it's possible to notice again the influence caused by the fluid flow in particles motion. The rotational valve had, before the particles reach the exit, raised the local pressure, making with that the first particles already moves to the clean water exit.

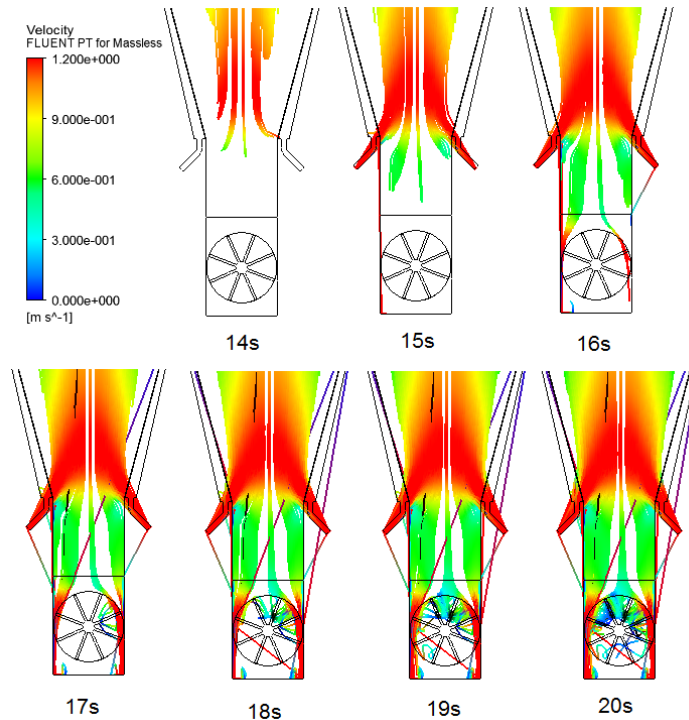


Figure 7. Particles velocity in the exit area

These results indicate a tendency to the particles exit only when they are near to the purified water exit, and that means that, when a physical prototype is built, must be considered that region of the porous media will be more saturated than other regions, indicating a necessity of a periodical cleaning to avoid a possible clog.

## 5. CONCLUSION

Comparing the fluid and particles behavior, was clear to notice the influence that the fluid phase causes in the particles in a one-way simulation. The analysis objective must be evaluated to considerer what kind of CFD-DEM coupling should be used, because a one-way simulation could not give precise results compared with a two way. For the present paper's simulation, the one-way consideration was plausible since only the visual interpretation of slurry flow was considered.

The restriction cause by the rotative valve force the fluid and particles to go through the porosity regions, making possible to create a particle filtering and expel a lower percentage particle in clean water. The regions of preference particles retention could be identified, indicating a cleaning improvement in that region while making the physical experiment.

The simulation provided an idea of the equipment's operations, but some considerations still must be made, like a comparison with an experimental analysis to validate the computational results. Looking for a more precise results, in future works is indicated that a mesh independence verification be executed, to guarantee no presence of mathematical errors, and also a two-way simulation be performed, what will indicate with more accuracy the fluid and particles track, while one interfere in the others motion.

## 6. ACKNOWLEDGEMENTS

To Pontificia Universidade Católica de Minas Gerais – PUCMINAS its employees and teachers, to Fundação de Amparo à Pesquisa do Estado de Minas Gerais – FAPEMIG, to Conselho Nacional de Desenvolvimento Científico e Tecnológico - CNPq and to Coordenação de Aperfeiçoamento de Pessoal de Nível Superior – CAPES, for the support and contributions related to the realization of this reseaches and article.

## 7. REFERENCES

ANSYS Fluent theory guide

- Fatahi M.R., A. Farzanegan. An analysis of multiphase flow and solids separation inside Knelson Concentrator based on four-way coupling of CFD and DEM simulation. *Minerals Engineering* vol. 126 p. 130–144, 2018
- Fernandes C., Semyonov D., Ferrás L. L, Miguel Nóbrega J.. Validation of the CFD-DPM solver DPMFoam in OpenFOAM through analytical, numerical and experimental comparisons. *Granular Matter*, 20:64, 2018.
- Fuping Qian, Naijin Huang, Jinli Lu, Yunlong Han. CFD–DEM simulation of the filtration performance for fibrous mediabased on the mimic structure. *Computers and Chemical Engineering* vol.71 p. 478–488, 2014
- Hall, C. W. Handbook of Industrial Drying. *Drying Technology*, v. 6, n. 3, p. 571–573, 1988.
- Hamelin, L. et al. Environmental consequences of future biogas technologies based on separated slurry. *Environmental Science and Technology*, v. 45, n. 13, p. 5869–5877, 2011.
- Januário, J. R., Maia, C. B. Modeling and numerical simulation of slurry flow. *Brazilian Journal of Development*, v. 5, n. 10, p. 20462–20477, 2019.
- Jorgensen, K. et al. Phosphorus distribution in untreated and composted solid fractions from slurry separation. *Journal of Environmental Quality*, v. 39, n. 1, p. 393–401, 2010.
- Lin, Y. C.; Tai, C. Y. Recovery of silicon powder from kerfs loss slurry using phase-transfer separation method. *Separation and Purification Technology*, v. 74, n. 2, p. 170–177, 2010.
- Luke Stone, David Hastie, Stefan Zigan. Using a coupled CFD – DPM approach to predict particle settling in a horizontal air stream. *Advanced Powder Technology* vol. 30 p. 869–878. 2019
- Ma, L. et al. Modeling of erodent particle trajectories in slurry flow. *Wear*, v. 334–335, p. 49–55, 2015.
- Mannheimer, R. J. Laminar and turbulent flow of cement slurries in large diameter pipe: A comparison with laboratory viscometers. *Journal of Rheology*, 35(1), 113–133. 1991.
- Mohammad A. Elyyan, Mai Doan, Yeong-Yan Perng. Fluid-structure interaction modeling of subseajumper pipe, *Proceedings of the ASME 2014 33<sup>rd</sup> International Conference on Ocean, Offshore and Arctic Engineering*, sdf

- Mujumdar, A. S. Research and development in drying: Recent trends and future prospects. *Drying Technology*, v. 22, n. 1–2, p. 1–26, 2004.
- NGUYEN, T. T.; INDRARATNA, B. Experimental and numerical investigations into hydraulic behaviour of coir fibre drain. *Canadian Geotechnical Journal*, v. 54, n. 1, p. 75–87, 2016.
- VERSTEEG, Henk Kaarle; MALALASEKERA, Weeratunge. An introduction to computational fluid dynamics: the finite volume method. Pearson education, 2007.
- YUE, C.; ZHANG, Q.; ZHAI, Z. Numerical simulation of the filtration process in fibrous filters using CFD-DEM method. *Journal of Aerosol Science*, v. 101, p. 174–187, 2016.

## **8. RESPONSIBILITY NOTICE**

The author(s) Matheus Dutra Baptista Oliveira and Cristiana Brasil Maia are the only responsible for the printed material included in this paper.